Moffatt Eddies in Viscous Flow Through a Curved Tube of Square Cross Section

A. McD. MERCER

Department of Mathematics and Statistics
University of Guelph
Guelph, Ontario, Canada

INTRODUCTION

When an incompressible viscous fluid passes through a curved tube of constant cross section the resulting velocity field can be considered as being made up of two components. There is a dominant basic flow perpendicular to the cross section of the tube and a secondary flow in the plane of this cross section. The latter is induced by the curvature of the tube. Let us consider this secondary flow. If the cross section possesses a corner of sufficiently small angle (less than about 146°) the analysis of Moffatt (1964) suggests that an infinite sequence of eddies should appear in this corner as part of the secondary flow. This aspect of tube flow has been investigated by Collins and Dennis (1976a) for the case of a triangular cross section with small Dean number, and these vortices have been found in the 90° and 45° corners. They are, furthermore, seen to persist for larger Dean numbers (Collins and Dennis, 1976b). Apart from these two investigations of the triangular cross section we know of no other case of this phenomenon having being studied. It is the purpose of this note to demonstrate the presence of these Moffatt eddies in the case of a square cross section for small values of the Dean number.

As is usual in such studies the problem will be discretized by covering the cross section with a square mesh. However, due to the small size of the corner eddies, this mesh needs to be refined considerably in the vicinity of the corners to obtain the necessary detail.

GOVERNING EQUATIONS

The Navier-Stokes equations of motion of a viscous fluid have been adapted to the present situation by Dean (1927, 1928); to save space we do not repeat the analysis here. In the present case the cross section is a square and we take the coordinate system shown in Figure 1. C is the center of curvature of the tube, R is a constant and, letting the half-side of the square be a we assume that $a << R$. A constant pressure gradient causes the motion and if this has the velocity components (u', v', w') in the directions of increasing (x', y', ϕ) we suppose that they are functions of x' and y' only. The problem is de-dimensionalized and a dimensionless stream function ψ for the secondary flow is introduced as follows:

$$x' = ax \qquad y' = ay \tag{1}$$

$$u' = \frac{\nu}{a}\frac{\partial \psi}{\partial y} \qquad v' = -\frac{\nu}{a}\frac{\partial \psi}{\partial x} \qquad w' = \frac{\nu}{a}\left(\frac{2a}{R}\right)^{-1/2} w$$

The continuity equation is now automatically satisfied. Then the third inertial equation and the first two inertial equations combined yield the following, respectively:

$$\left.\begin{aligned} \nabla^2 w + \psi_x w_y - \psi_y w_x &= -D \\ \nabla^4 \psi + \psi_x (\nabla^2 \psi)_y - \psi_y (\nabla^2 \psi)_x + w w_y &= 0 \end{aligned}\right\} \tag{2.1}$$

In the foregoing $\nabla^2 \equiv (\partial^2/\partial x^2) + (\partial^2/\partial y^2)$, ν is the kinematic viscosity, and D is the Dean number:

$$D \equiv Ga^3 (2a/R)^{1/2} \rho^{-1} \nu^{-2}$$

where ρ is the density. We have chosen to define the Dean number in this way to conform to that used by Collins and Dennis (1976a) for the triangular section.

The appropriate boundary conditions for Eq. 2.1 are

$$w = \psi = \psi_\mu = 0 \quad \text{on} \quad \Gamma \tag{2.2}$$

where Γ is the boundary of the nondimensional square cross section. This section now has side length 2 (i.e., $PQ = QR =$

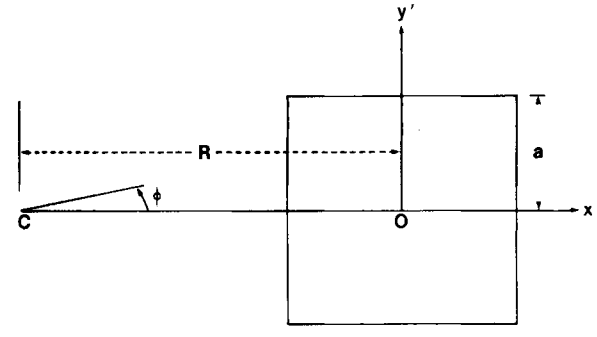

Figure 1. The coordinate system.

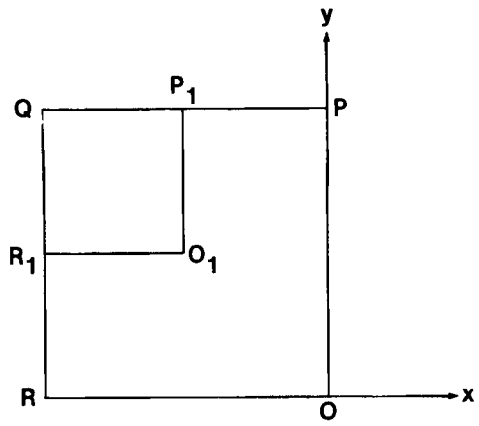

Figure 2. Notation for the cross section.

1 in Figure 2). Here the suffix μ denotes $\partial/\partial\mu$, differentiation in the direction normal to Γ.

As $D \to 0$, clearly both $w \to 0$ and $\psi \to 0$. Following Dean, if we suppose that w and ψ can be expanded as power series in D, for sufficiently small D we can calculate the successive coefficients of these power series by substitution in Eq. 2.1. One easily finds that as $D \to 0$

$$w = DW + O(D^3)$$
$$\psi = D^2\Psi + O(D^4)$$

where W and Ψ satisfy

$$\left.\begin{aligned} \nabla^2 W &= -1 \\ \nabla^4 \Psi &= -WWy \end{aligned}\right\} \tag{2.3}$$

with $W = \Psi = \Psi_\mu = 0$ on Γ

It will be convenient to introduce a third function, Ω so that finally our problem takes the form:

$$\left.\begin{aligned} \nabla^2 W &= -1 \\ \nabla^2 \Omega &= WWy \\ \nabla^2 \Psi &= -\Omega \end{aligned}\right\} \tag{2.4}$$

with $W = \Psi = \Psi_\mu = 0$ on Γ (2.5)

Before proceeding to describe the numerical treatment of the problem we shall make some use of symmetry. Clearly W will be an even function in both x and y, Ω will be even in x but odd in y, and then Ψ will have the same character as Ω. Hence we can limit our attention to (say) the top left quarter of the square section, Figure 2. The boundary conditions for this quarter square are

$$\left.\begin{aligned} W_x = \Psi_x = \Omega_x &= 0 \quad \text{on} \quad OP \\ W = \Psi = \Psi_y &= 0 \quad \text{on} \quad PQ \\ W = \Psi = \Psi_x &= 0 \quad \text{on} \quad QR \\ W_y = \Psi = \Omega &= 0 \quad \text{on} \quad RO \end{aligned}\right\} \tag{2.6}$$

NUMERICAL TREATMENT

Our numerical procedure for solving the problem of Eqs. 2.4 and 2.6 follows that of Collins and Dennis (1976a). The square $OPQR$ (Figure 2) is covered by a square mesh of side h, lines of the mesh coinciding with edges of the square. Using the familiar notation in which the points (x_o, y_o), $(x_o + h, y_o)$, $(x_o, y_o + h)$, $(x_o - h, y_o)$, $(x_o, y_o - h)$ are denoted by suffices 0,1,2,3,4, respectively, Eqs. 2.4 are replaced by the three systems of linear algebraic equations:

$$\left.\begin{aligned} \sum_1^4 W_i - 4W_o &= -h^2 \\ \sum_1^4 \Omega_i - 4\Omega_o &= \frac{h}{2} W_o(W_2 - W_4) \\ \sum_1^4 \Psi_i - 4\Psi_o &= -h^2\Omega_o \end{aligned}\right\} \tag{3.1}$$

Once the boundary conditions, Eq. 2.6, are translated into the corresponding edge conditions for the three sets of Eq. 3.1, we can proceed to solve these sets numerically. The set for W can be solved once and for all. When W is found at the nodes of the mesh we can then alternately solve the sets for Ω and Ψ, this iteration being continued until convergence according to some criterion is achieved. It should be mentioned here that although the last two sets in Eq. 3.1, corresponding to the last two of Eq. 2.4, do not appear to be cross-coupled, in fact they are due to the boundary conditions applying to them; see Eqs. 3.2 and 3.3 below. In each of these calculations the SOR technique is found to be satisfactory. As to the edge conditions applying to each of these sets of Eq. 3.1, we note the following.

Due to symmetry about the line OQ the set for W can be solved merely on the triangle OQR. We see from Eq. 2.6 that $W_o = 0$ on QR and $W_2 = W_4$ if (x_o, y_o) is on RO. Then by symmetry, if (x_o, y_o) is on OQ we have $W_2 = W_3$ and $W_1 = W_4$.

From Eq. 2.6 the edge conditions pertaining to Ψ are seen at once to be $\Psi_o = 0$ on PQ,QR,RO while $\Psi_1 = \Psi_3$ if (x_o, y_o) is on OP.

Turning to the function Ω some care must be exercised, as noted by Collins and Dennis (1976a). From Eq. 2.6 we see immediately that $\Omega_o = 0$ on RO and $\Omega_1 = \Omega_3$ if (x_o, y_o) is on OP. But edge conditions on PQ and QR have still to be obtained. Since the equations in 3.1 all have truncation errors of order h^4 we need to obtain approximations to the edge conditions for Ω of this same order. Let (x_o, y_o) be a point on QR, for example. From Eq. 2.6 we have $\Psi_o = \Psi_2 = \Psi_4 = (\Psi_x)_o = 0$. Hence the last of Eq. 3.1 yields

$$\Psi_1 + \Psi_3 = -h^2\Omega_o + O(h^4)$$

Also, from the Taylor series for $\Psi(x_o \pm h, y_o)$ we get

$$\Psi_1 - \Psi_3 = \frac{1}{3} h^3(\Psi_{xxx})_o + O(h^5)$$

Now the last of Eq. 2.4 and the Taylor series for $\Omega(x_o + h, y_o)$ give

$$(\Psi_{xxx})_o = -(\Omega_x)_o \quad \text{and} \quad (\Omega_x)_o = (1/h)(\Omega_1 - \Omega_o) + O(h)$$

From these four equations we get, to order h^4

$$\Omega_o = -\frac{3}{h^2}\Psi_1 - \frac{1}{2}\Omega_1 \quad \text{if} \quad (x_o, y_o) \quad \text{is on} \quad QR \tag{3.2}$$

Similarly we find

$$\Omega_o = -\frac{3}{h^2}\Psi_4 - \frac{1}{2}\Omega_4 \quad \text{if} \quad (x_o, y_o) \quad \text{is on} \quad PQ \tag{3.3}$$

Initially some numerical experiments were carried out to determine the required mesh size. The difference equations for W were solved in the triangle OQR using mesh sizes h = 1/10, 1/20, 1/40, 1/80. The mesh h = 1/40 gave the converged value of W to within one unit in the fourth significant figure. Next, with mesh sizes h = 1/10, 1/20, 1/40 the difference equations for Ω and Ψ were solved. Applying Richardson ex-

trapolation (Smith, 1969) it was found that the values of Ψ along the two center lines of the square $OPQR$ had converged to within a relative error of 0.2%. It was therefore decided to use the 1/40 mesh size for all subsequent calculations.

The general procedure used was to calculate the three functions W, Ω, Ψ inside a sequence of squares obtained from $OPQR$ by successive bisection, proceeding into the corner Q. These squares can be denoted by $O_nP_nQR_n$ where, for example, R_1 bisects QR and O_n is the center point of the nth square, $OPQR$ being the first one (see Figure 2).

Once these three functions are obtained in $OPQR$ on a 40 $\times$ 40 mesh they will be known in $O_1P_1QR_1$ on a 20 $\times$ 20 mesh. This is now refined to a 40 $\times$ 40 mesh using a highly accurate interpolation method along the sides $R_1O_1P_1$ and linear interpolation elsewhere in $O_1P_1QR_1$. (At these latter points all that is needed is a first approximation to the functions to be used in the subsequent iterations.) The difference equations for W, Ω, Ψ are now solved in $O_1P_1QR_1$ as before except that now, of course, the boundary conditions along the edges $R_1O_1P_1$ are in all cases the values of the respective functions as obtained from the previous calculations.

This technique was repeated several times until finally we had obtained the values of the three functions on a 40 $\times$ 40 subdivision of $O_8P_8QR_8$. This corresponded to a subdivision of the whole cross section of the tube of size 20,480 $\times$ 20,480. At this stage the first two Moffatt eddies were obtained in detail.

In each successive overrelaxation used throughout the calculations the relaxation factor of 1.6 was found to be satisfactory. The iterative process which successively calculated Ω and Ψ was repeated in each case until there was no change to a tolerance well within the accuracy range expected of the solutions. As regards the boundary conditions on P_nQR_n for the function Ω, these were recalculated at each stage according to the scheme.

$$\Omega_o^{(k+1)} = \gamma\left[-\frac{3}{h^2}\Psi_1^{(k)} - \frac{1}{2}\Omega_1^{(k)}\right] + (1-\gamma)\Omega_o^{(k)} \quad \text{on} \quad QR_n$$

$$\Omega_o^{(k+1)} = \gamma\left[-\frac{3}{h^2}\Psi_4^{(k)} - \frac{1}{2}\Omega_4^{(k)}\right] + (1-\gamma)\Omega_o^{(k)} \quad \text{on} \quad P_nQ$$

using the factor $\gamma = 0.05$.

At each stage also, as a check on the accuracy of Ψ, values of this function at points common to consecutive squares were compared. These comparisons were very satisfactory. In view of the maximum possible relative error of 0.2% in the values of Ψ along the sides $R_1O_1P_1$, it would appear that the accuracy of the calculated values of Ψ in the square $O_8P_8QR_8$ is within 2% in relative error.

It would now be possible to continue this process, proceeding to a yet finer mesh in the vicinity of the corner Q. We could then obtain the third, fourth, and succeeding Moffatt eddies in the corner, achieving less accuracy, of course, as we proceeded. Indeed, in Collins and Dennis (1976a) no fewer than thirteen of these eddies have been obtained in one of the corners of the triangular cross section. In the present case, however, we have not proceeded beyond the second eddy.

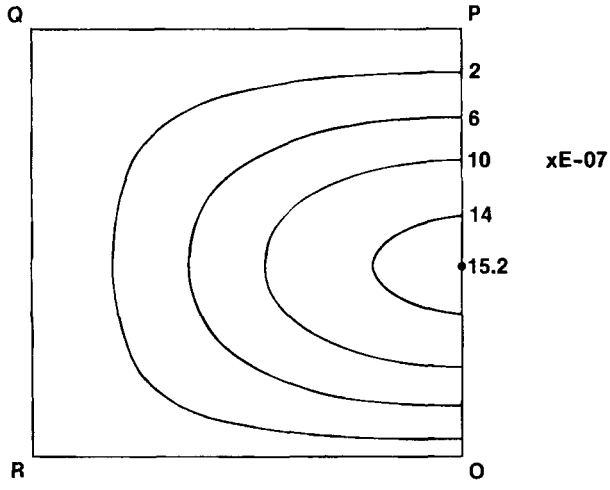

Figure 3. Secondary flow stream lines on *OPQR*.

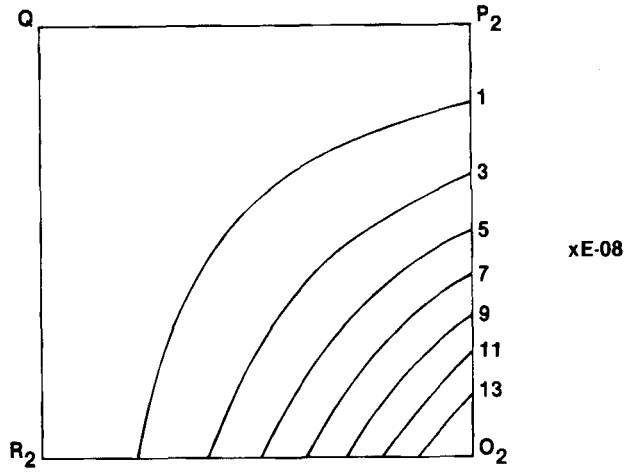

Figure 4. Secondary flow stream lines on $O_2P_2QR_2$.

RESULTS

Our results are presented graphically in Figures 3 to 7, which illustrate the streamlines in $OPQR$ and in $O_nP_nQR_n$ for n = 2,4,6,8, respectively.

Let us call that point of a Moffatt eddy at which Ψ = constant is itself a single point, the center of the eddy. Then if γ_n denotes the distance of the center of the nth Moffatt eddy from the corner Q, Moffatt's similarity analysis, which treats the sides RO and OP as being at infinity yields the results:

$$\left|\frac{\gamma_n}{\gamma_{n+1}}\right| \sim \exp\left(\frac{\pi^2}{2\eta_n}\right) \text{ and } \left|\frac{\Psi_{\gamma_n}}{\Psi_{\gamma_{n+1}}}\right| \sim \left|\frac{\gamma_n}{\gamma_{n+1}}\right|^{2\xi_n/\pi+1}$$

($\eta_1 = 1.758$, $\xi_1 = 4.303$ in our case.)

For the details of these results we refer the reader to Collins and Dennis (1976a) and Moffatt (1964).

In the present case these values can be expected to be approximated only for large n but, in fact, we notice that using only the first two eddies we obtain the following comparisons:

Ratio	Moffatt	Present
$\left\|\gamma_1/\gamma_2\right\|$	16.56	16.94
$\left\|\Psi_{\gamma_1}/\Psi_{\gamma_2}\right\|$	3619	3650

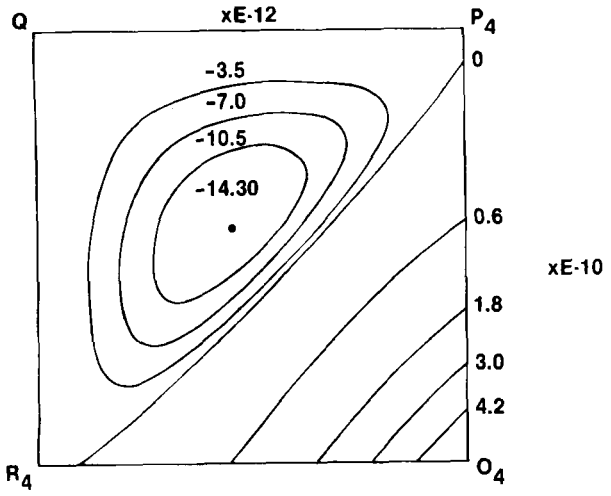

Figure 5. Secondary flow stream lines on $O_4P_4QR_4$.

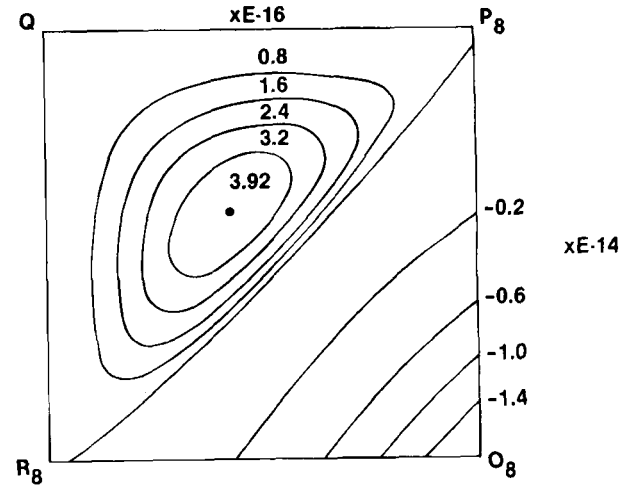

Figure 7. Secondary flow stream lines on $O_8P_8QR_8$.

These results compare surprisingly well since they refer only to the first two eddies, whereas Moffatt's formulae above are asymptotic as $n \to \infty$ when applied to the present problem. Possibly the situation is aided by the fact that the form of the main secondary vortex near Q, Figure 3, has something of the form of a Moffatt eddy itself.

NOTATION

a = half-side of the square section
D = Dean number = $Ga^3(2a/R)^{1/2}\rho^{-1}\nu^{-2}$
G = pressure gradient
h = mesh size
p = pressure
R = radius of curvature of the tube
γ_n = distance of the nth Moffatt eddy from the corner
(u', v', w') = velocity components
W, Ψ = functions proportional to w and ψ, respectively, when D is small
w = dimensionless axial velocity
(x', y', ϕ) = coordinate system
(x, y, ϕ) = dimensionless coordinate system
γ = relaxation factor for the boundary conditions for Ω
Ψ_{γ_n} = value of Ψ at the center of the nth Moffatt eddy
ψ = dimensionless stream function
ρ = density
ν = kinematic viscosity
Ω = auxiliary function, Eq. 2.4

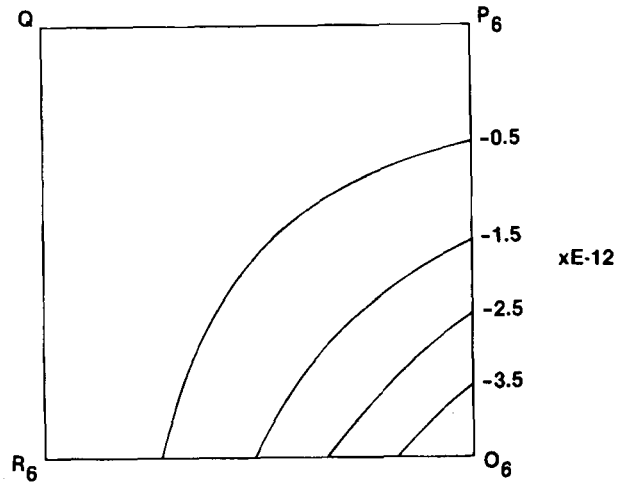

Figure 6. Secondary flow stream lines on $O_6P_6QR_6$.

LITERATURE CITED

Collins, W. M., and S. C. R. Dennis, "Viscous Eddies Near a 90° and a 45° Corner in Flow Through a Curved Tube of Triangular Cross Section," *J. Fluid Mech.*, **76**, 417 (1976a).

———, "Steady Flow in a Curved Tube of Triangular Cross Section," *Proc. Roy. Soc., Ser. A*, **352**, 189 (1976b).

Dean, W. R., "Note on the Motion of Fluid in Curved Pipes," *Phil. Mag.*, **4**(7), 208 (1927).

———, "The Streamline Motion of Fluid in a Curved Pipe," *Phil. Mag.*, **5**(7), 673 (1928).

Moffatt, H. K., "Viscous and Resistive Eddies Near a Sharp Corner," *J. Fluid Mech.*, **18**, 1 (1964).

Smith, G. D., *Numerical Solution of Partial Differential Equations*, Oxford Univ. Press (1969).

Manuscript received Nov. 5, 1984, and revision received June 4, 1985.